THE SPARC_LAB THOMSON SOURCE COMMISSIONING

C. Vaccarezza, D. Alesini, M. P. Anania, M. Bellaveglia, E. Chiadroni, D. Di Giovenale, G. Di Pirro, M. Ferrario, A. Gallo , G. Gatti, R. Pompili, S. Romeo, F. Villa, INFN-LNF, Frascati, Italy
A. Cianchi, University of Rome Tor Vergata and INFN
P. Oliva, B. Golosio, Dip. Di Fisica, University of Sassari and INFN-Cagliari, Italy
M. Gambaccini, P. Cardarelli, G. Di Domenico, University of Ferrara and INFN-FE, Ferrara, Italy
P. Delogu University of Pisa and INFN-Pisa, Pisa, Italy
A. Bacci, C. Curatolo, D. Palmer, V. Petrillo, A. R. Rossi, L. Serafini, P. Tomassini INFN-Milano, Milano, Italy
A. Giribono, F. Filippi, A, Mostacci, Università La Sapienza, Roma, Italy

Abstract

The SPARC_LAB Thomson source is presently under commissioning at LNF. An electron beam of energy between 30-150 MeV collides head-on with the laser pulse provided by the Ti:Sapphire laser FLAME, characterized in this phase by a length of 6 ps FWHM and by an energy ranging between 1 and 5 J. The key features of this system are the wide range of tunability of the X-rays yield energy, i.e. 20-500 keV, and the availability of a coupled quadrupole and solenoid focusing system, allowing to reach an electron beam size of 10-20 microns at the interaction point. The experimental results obtained in the February 2014 shifts are presented.

INTRODUCTION

Radiation sources based on the Thomson backscattering effect have become more and more attractive due the large variety of applications in biological, medical and industrial science and relatively compactness of the whole apparatus. At the Frascati INFN-SPARC_LAB [1] the opportunity has been used to couple the SPARC High Brightness photoinjector [2] with the 250 TW FLAME laser system [3] in order to provide a X-ray Thomson source in the range of 20-500 keV. A 20 m double dogleg carries the electron beam output from the photoinjector down to the Thomson Interaction Point where the FLAME laser pulse is brought by a 20 m in vacuum optical transfer line, see Fig. 1. The parameters of the electron and laser beams, reported in Table 1, have been optimized in view of the first planned experiment with the Thomson radiation: the X-ray imaging of mammographic phantoms with phase contrast technique [4,5], requiring high flux of photons and moderate monochromaticity.

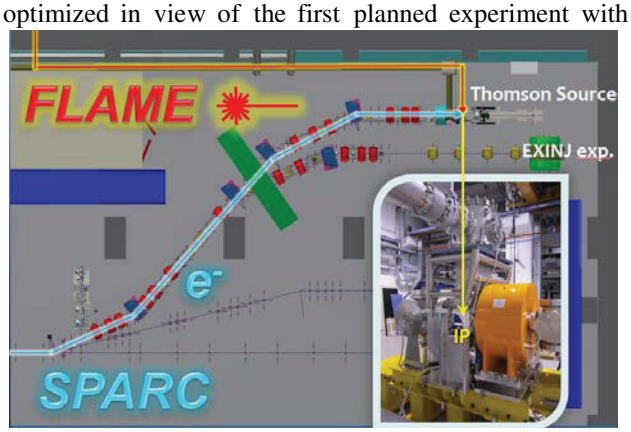

Figure 1: SPARC_LAB Thomson source schematic layout.

Table 1: Thomson Source Design Parameters

Electron Beam	Energy	(MeV)	30÷150
	Energy spread	(%)	<0.1
	Charge	(pC)	100-800
	Emittance	(mm mrad)	1÷3
Laser Beam	Wavelength	(nm)	800
	Pulse energy	(J)	1÷5
	Pulse length	(ps)	6
	Spot size	(μm)	10
	Repetition rate	(Hz)	10
X-ray Beam	Photon energy	(keV)	20-500
	Photon number per shot		10^9
	Source rms radius	(μm)	10
	Bandwidth	(%)	10

THE ELECTRON BEAM

The electron beam is provided by a 1.6 cell S-band RF gun equipped with a Cu photocathode driven by a 50 μJ Ti:Sapphire laser and a four coils solenoid for the emittance compensation. The beam is then accelerated by three TW SLAC type S-band linac sections (S1-S3) up to the desired energy. At the exit of the linac a 6D beam phase space measurement system is available [6] by means of a S-band RF deflecting cavity and a 14° bypass dipole employed also for energy and energy spread measurements.

For the commissioning phase a low charge working point has been set up with Q= 200 pC beam and energy E= 50 MeV; the phases of the accelerating sections have been chosen as follows: Φ_{S1}=-26.2°, Φ_{S2}= +78.5, Φ_{S3}= -111° from crest, in order to minimize the effects of the power amplitude jitter from the feeding Klystrons.

ISBN 978-3-95450-132-8

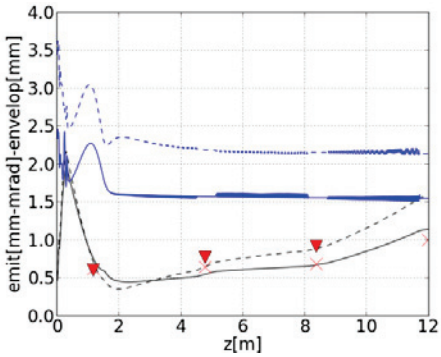

Figure 2: Electron beam emittance (blue curves) and envelope evolution (black curves) from the photocathode to the linac exit calculated with the Astra code. The dots represent the beam spot measurements taken in this configuration at screen locations along the linac.

The beam emittance and envelope evolution through the photoinjector has been simulated with the ASTRA code [7] and 50k particles; the results are shown in Fig. 2 together with the beam spot measurements taken at the screen locations along the linac. From the photoinjector exit a double dogleg with a final two branch interaction zone brings the electron beam to the interaction points of the Thomson and the plasma acceleration external injecton experiment [1], see Fig. 1. The R_{56} parameter can be set in the range of ± 50 mm, closing the horizontal dispersion at the end of the last dipole (Fig. 3). For the commissioning phase the dispersion is closed at the end of each dipole pair and the emittance evolution measurement is performed with the quadrupole scan technique in each straight section downstream the dipole pairs.

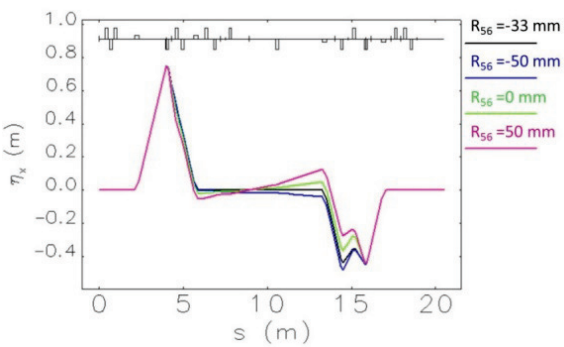

Figure 3: Double dogleg R_{56} tunability and relative horizontal dispersion plot.

From the transverse emittance measurement performed at the linac exit the Twiss parameters are obtained to match the beam to the dogleg entrance for the transport and focusing at the Thomson Interaction Point. The space charge effects are included in the TRACE3D code [8] used for the beam matching.

For the commissioning a working point has been chosen with Q=200 pC and energy E=50 MeV, the calculated Twiss parameters evolution up to the Thomson Interaction Point are shown in Fig. 4.

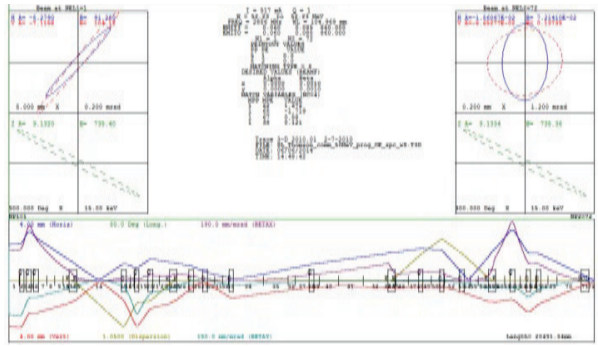

Figure 4: Twiss parameters and envelope evolution from the linac exit to the Thomson IP obtained with the TRACE3D code.

THE PHOTON BEAM

The laser pulse used to drive the Thomson back scattering process with the SPARC electron beam is provided by the FLAME laser system [2]. Briefly FLAME is a nominal 300 TW laser system that uses 11 YAG pump lasers and 5 titanium-sapphire multi-pass amplifiers to produce linearly polarized pulses with a central wavelength λ_0=0.800 µm in a 60÷80 nm bandwidth. The pulse duration ranges between 25 fs ≤ τ_L ≤ 10 ps, and the maximum energy is E= 7J that corresponds to an energy on target E_t ~ 5J, at 10 Hz repetition rate. The laser system is hosted in a clean room at the ground floor of the FLAME building and is optically transported in a shielded underground area where the compressor is located and that is adjacent to the SPARC hall. From here an optical transfer line in vacuum, (P=10^{-6} Torr), carries the beam up to the parabolic mirror of the Thomson interaction chamber (Fig. 5) that focuses the beam in a 10 µm diameter (FWHM) spot at the interaction point.

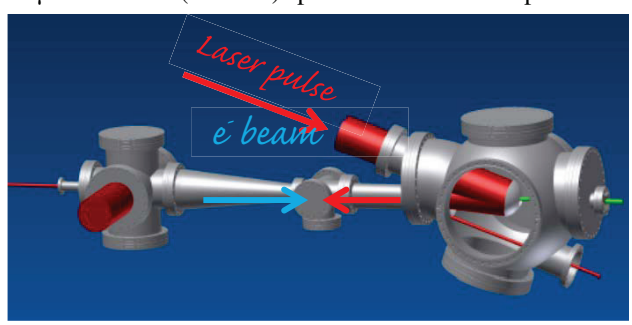

Figure 5: 3D CAD drawing of the Thomson Interaction vacuum chamber setup.

X-RAY BEAM DIAGNOSTIC

In the commissioning phase, the x-ray detection is a fundamental diagnostic tool to verify the collision alignment and synchronisation. In this phase a detector that allows to measure the x-ray yield is required that must have a high sensitivity and a wide dynamic range to detect the potentially weak signal generated in the first non-optimised collisions. The detector we selected is a scintillator crystal coupled with a photomultiplier tube (PMT). The crystal used is a CsI(Tl) of size (20x20x2) mm^3, coupled with a light-guide to a PMT (Hamamatsu,

mod. R329-02). The signal is acquired using both an oscilloscope and a multichannel analyser (MCA-8000, Amptek, US) connected to a PC. Due to the high intensity and short duration of the pulse, it is not possible to distinguish the signal produced by the interaction of each single photon in a pulse, as in traditional spectroscopic application, but the signal is proportional to the entire energy released in the scintillator by each pulse. Therefore, an information on the energy distribution is required to evaluate the number of photon in each pulse.

To calibrate the detector response, the signal produced by two radioactive sources: Am-241 (59.54 keV) and Cs-137 (662 keV) was performed as a function of the HV applied and the amplificator gain; adjusting the HV and gain it is possible to detect signals in a wide range. For a monochromatic radiation at 60 keV, it is possible to detect the signal produced by a single photon up to the one due to pulses containing about 10^6 photons. The detector was placed at a distance of 4 m from the IP, aligned with the x-ray propagation direction and mounted on an *x-y* movement for the fine position adjustment. In addition to the PMT described, the beamline is equipped with a set of detectors that, together with techniques specifically developed [9-10], will allow a full characterization of the x-ray source in terms of flux, energy distribution, spatial distribution and beam stability, during the next 2014 run.

COMMISSIONING RESULTS

For the commissioning phase a 200 pC electron beam at 50 MeV has been selected as working point. At the Linac exit the measured normalized transverse emittance was $\varepsilon_{x\text{-}y}$ = 1.5 - 2.2 ± 0.2 mm mrad, with an energy spread σ_δ= 0.1 ± 0.03 %, and a rms length σ_z = 3.1 ± 0.2 ps. In this very first four weeks shift the focusing solenoid upstream the IP was kept at 70 % of the nominal value due to a limit in the magnet cooling system for which an upgrade is foreseen in the June 2014 shutdown. The minimum electron beam size reached was $\sigma_{x\text{-}y}$ ~ 90 ± 3 µm, nevertheless a clear Thomson photon production signature has been obtained with an electron spot size $\sigma_{x\text{-}y}$ ~ 240-160 ± 10 µm, due to a residual misalignment and a consequent poor overlap between the electron and laser beams that have to be recovered for the next run.

Simulations of the interaction between the electron beam and the laser pulse have been made with a code

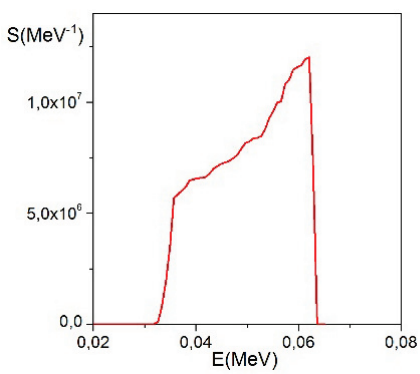

Figure 6: Spectral density S (MeV^{-1}) versus photon energy.

based on the classical theory [11]. The 50 MeV electron beam, with 200 pC charge, 5 mm mrad of emittance, 150 µm of rms beam transverse dimension, colliding with the laser with 500 mJ and 30 µm of waist, gives a number of photons of 2×10^5 in a bandwidth of about 19%. The photon energy edge, given by $E_p \sim 4E_L \gamma^2$, is about 63 keV. Figure 6 shows the spectral density S in MeV^{-1} vs the photon energy in MeV.

The signal of the x-ray detector was measured using both a 20 GHz bw oscilloscope, for a fast response, and the multichannel analyser to acquire an integral measurement over various interactions. In Fig. 7 the results of the multichannel acquisition are shown as a histogram of the signal intensities acquired over 120 s; it is possible to distinguish the signal due to background (without interacting laser FLAME) and that due to Thomson backscattering. The pulse-to-pulse variation is due to fluctuations of the overlap region of the two beams, the relative temporal jitter between electrons and photons is ~150 fs.

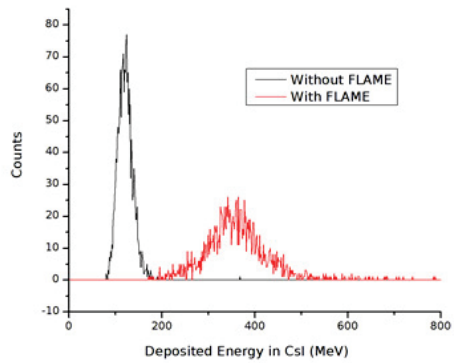

Figure 7: Thomson x-rays signal in red, in black the electron background signal (without FLAME laser), integrated over 120 s (1200 pulses).

The obtained signal is the sum of the background and the signal due to Thomson X-rays: performing a background subtraction it results in an average energy of about 235 MeV released in the crystal by each pulse. This background is synchronous to the Thomson x-rays and it is mainly due to the radiation produced in the electron beam dumping section being the dumping dipole presently located downstream the parabolic mirror vacuum chamber, i.e. too much close to the X-ray radiation extraction. In the June 2014 shutdown the insertion is foreseen of a dumping dipole immediately after the interaction point, to avoid any background contribution from the dumping beam line.

The energy distribution of the Thomson radiation was reconstructed by CAIN simulation of the interaction and the average energy of the photons reaching the detector was 60 keV. We can then calculate that the number of photons per each pulse, nevertheless coming from poor overlap conditions, and interacting with the detector sensitive area, is in average $6.7\text{x}10^3$. In the next 2014 run a full characterization of the source is planned, including also the measurement of the energy distribution and the spatial distribution of the radiation produced.

ISBN 978-3-95450-132-8

REFERENCES

[1] M. Ferrario et al., Nucl. Instrum. Methods B 309, 183 (2013).
[2] M. Ferrario et al., "Advanced Beam Dynamics Experiments with the SPARC High Brightness Photoinjector", TUPE082, IPAC 10, Kyoto, Japan (2010).
[3] L. Labate et al., Radiat. Eff. Def. Solids 165, 787 (2010).
[4] A. Bacci et al., Nucl. Instrum. Methods A 608, S90 (2009).
[5] P. Oliva et al., Nucl. Instrum. Methods A 615, 93 (2010).
[6] D. Alesini et al., Nucl. Instrum. Methods A 568, 488 (2006).
[7] K. Flottmann, http://www.desy.de/~mpyflo/
[8] K. R. Crandall, D. P. Rusthoi, LA-UR-97-886 (1997).
[9] P. Cardarelli et al., J. Appl. Phys. 112, 074908 (2012).
[10] B. Golosio, Appl. Phys. Lett. 100, 164104 (2012).
[11] V. Petrillo et al., Nucl. Instrum. Methods A 693, 109 (2012).